PNAS RESEARCH ARTICLE | MICROBIOLOGY

Utilization of diverse organophosphorus pollutants by marine bacteria

Dragana Despotović[a,1], Einav Aharon[a,2], Olena Trofimyuk[a,2], Artem Dubovetskyi[a,b,2], Kesava Phaneendra Cherukuri[a,2], Yacov Ashani[a], Or Eliason[c], Martin Sperfeld[c], Haim Leader[a], Andrea Castelli[d], Laura Fumagalli[d], Alon Savidor[e], Yishai Levin[e], Liam M. Longo[f,g,1], Einat Segev[c,1], and Dan S. Tawfik[a,3]

Edited by Edward DeLong, University of Hawaii at Manoa, Honolulu, HI; received March 3, 2022; accepted June 17, 2022

Anthropogenic organophosphorus compounds (AOPCs), such as phosphotriesters, are used extensively as plasticizers, flame retardants, nerve agents, and pesticides. To date, only a handful of soil bacteria bearing a phosphotriesterase (PTE), the key enzyme in the AOPC degradation pathway, have been identified. Therefore, the extent to which bacteria are capable of utilizing AOPCs as a phosphorus source, and how widespread this adaptation may be, remains unclear. Marine environments with phosphorus limitation and increasing levels of pollution by AOPCs may drive the emergence of PTE activity. Here, we report the utilization of diverse AOPCs by four model marine bacteria and 17 bacterial isolates from the Mediterranean Sea and the Red Sea. To unravel the details of AOPC utilization, two PTEs from marine bacteria were isolated and characterized, with one of the enzymes belonging to a protein family that, to our knowledge, has never before been associated with PTE activity. When expressed in *Escherichia coli* with a phosphodiesterase, a PTE isolated from a marine bacterium enabled growth on a pesticide analog as the sole phosphorus source. Utilization of AOPCs may provide bacteria a source of phosphorus in depleted environments and offers a prospect for the bioremediation of a pervasive class of anthropogenic pollutants.

anthropogenic organophosphorus compounds | marine bacteria | phosphotriesterases | bioremediation

Significance

Marine bacteria are exposed to a range of industrial pollutants. Many of these compounds contain phosphorus, a key limiting nutrient in some marine environments. Yet it remains unknown whether bacteria utilize these environmental contaminants, especially because utilization requires a specialized enzyme called phosphotriesterase (PTE). We show that various common marine bacteria can thrive when organophosphorus pollutants are the sole phosphorus source, suggesting the presence of unidentified PTEs. Two new PTEs from marine bacteria were isolated and a strain of *Escherichia coli* that can thrive on organophosphorus compounds was engineered. We suggest that the ability to metabolize organophosphorus pollutants could be a competitive advantage for bacteria and a prospect for bioremediation.

Phosphorus (P) is an essential component of many key biological metabolites and is thus competitively utilized, particularly in marine environments, which can be P limited (1, 2). Microbial uptake of P preferentially occurs through phosphate or phosphate-containing natural metabolites—mainly phosphomonoesters, but also phosphodiesters and, to a lesser extent, phosphonates and phosphites (3). However, not all microorganisms can utilize all phosphorus sources (2, 4, 5) because multiple, specialized enzymes are required (Fig. 1). With the advent of industrialization, modern environments now have an additional source of P: anthropogenic organophosphorus compounds (AOPCs), which include phosphotriesters as well as diesters of both phosphonates and phosphites (6). These man-made compounds are used in an array of applications: phosphotriesters are pesticides (7), flame retardants (8) and plasticizers (9), while phosphonate diesters can act as potent nerve agents (10). Over the past several decades, AOPC pollutants have been identified in marine waters across the planet (11–13) and can potentially exceed the concentration of phosphate in P-depleted environments (1, 11) raising the question: Are AOPCs a viable alternative P source in environments with limiting concentrations of labile phosphorus?

As a potential nutrient for bacteria, AOPCs have some favorable properties: First, they can be hydrophobic, which may promote diffusion across membranes. Second, natural P sources are competitively utilized; thus, if AOPC utilization is a specialized trait, it may confer a fitness advantage. Unlike phosphodiesterases (PDEs) and phosphatases, phosphotriesterases (PTEs), which convert AOPCs into metabolically labile phosphodiesters and monophosphonate esters, have been detected in only a handful of soil bacteria that degrade the common pollutants paraoxon and Tris(2-chloroethyl) phosphate (14, 15). Several recent reports have noted indications of microbial utilization of AOPCs in seawater, such as stimulated growth upon addition of organophosphorus flame retardants (16, 17), PTE activity when the growth medium was supplemented with methyl paraoxon (17), and the observation of an alkaline phosphatase from *Alteromonas mediterranea* that can promiscuously act as a PTE (18), but it still remains unclear whether AOPCs, in the absence of another P source, can support microbial growth. To address this question, and uncover the biochemical details of AOPC metabolism, we systematically assayed the growth potential of model marine bacteria and environmental isolates on media containing a variety of AOPCs as the sole P source. We observed that 20 strains of marine bacteria can thrive under these conditions. Two PTE enzymes were isolated and exhibited

The authors declare no competing interest.

This article is a PNAS Direct Submission.

[1]To whom correspondence may be addressed. Email: dragana.despotovic@weizmann.ac.il, einat.segev@weizmann.ac.il, or llongo@elsi.jp.

[2]E.A., O.T., A.D., and K.P.C. contributed equally to this work.

[3]Deceased May 4, 2021, during the preparation of this manuscript.

This article contains supporting information online at http://www.pnas.org/lookup/suppl/doi:10.1073/pnas.2203604119/-/DCSupplemental.

Published August 2, 2022.

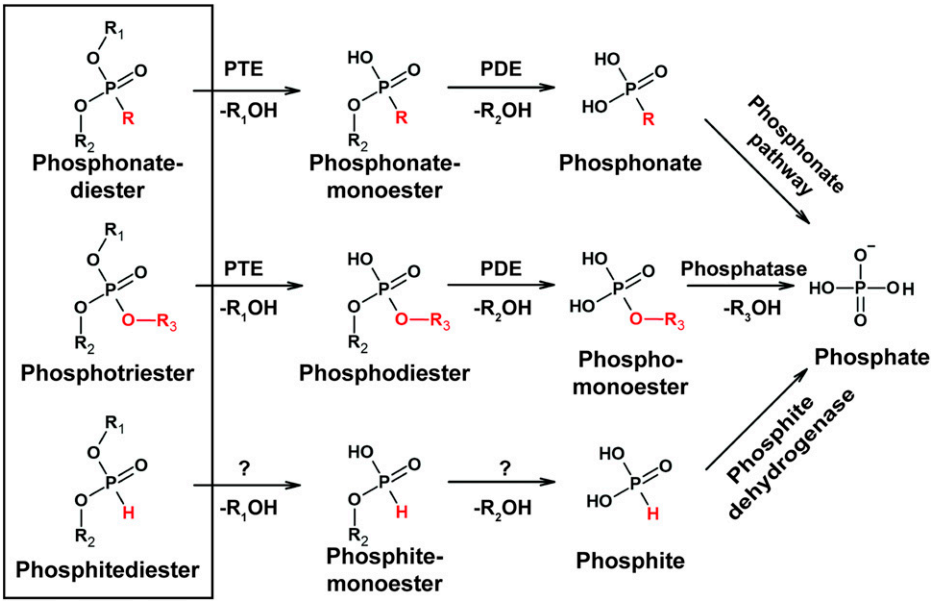

Fig. 1. Utilization pathways of AOPCs. AOPCs, indicated by a black rectangle, include phosphotriesters and their phosphonate and phosphite diester analogs. AOPCs share a similar structure, with the exception of the groups colored red. PTEs hydrolyze AOPCs to phosphodiesters and phosphonate monoesters, which are further hydrolyzed by PDEs. Enzymatic degradation of phosphite diesters is not yet well described, though it is suspected to involve PTEs and PDEs. The last step in the AOPC utilization pathway, conversion to phosphate, is mediated by three different enzymes: phosphatases hydrolyze phosphomonoesters to phosphate, C-P lyase and/or PhnY*/PhnZ oxygenases convert phosphonates to phosphate, and phosphite dehydrogenase converts phosphite to phosphate.

second-order rate constants (k_{cat}/K_M) that are on par with the average of all known phosphoesterases (mono, di-, and triphosphoesterases). When an AOPC utilization pathway was engineered into *Escherichia coli*, robust growth on AOPCs was observed. Taken together, these data demonstrate that bacteria can metabolize AOPCs, and they reveal that marine ecosystems are a reservoir for AOPC-utilizing enzymes.

Results and Discussion

Isolation of AOPC-Utilizing Marine Bacteria. The chemical properties of the R groups in AOPCs are diverse and tuned for specific applications. For example, pesticides and nerve agents are often designed with good leaving groups (i.e., conjugate acids with a low pK_a), while plasticizers and flame retardants, on the other hand, often bear poor leaving groups. As for R-group size, flame retardants, in particular, range from bulky to compact, depending on the industrial process. Phosphotriester derivatives are also commonly used: thiophosphates (P=S) and alkyl thiols (P-S-alkyl) are pesticides (and nerve agents), while phosphite diesters stabilize plastics. Thus, to broadly sample the chemical space of modern AOPCs as a potential P source, we used 15 representative AOPCs with diverse chemical properties (*SI Appendix*, Fig. S1 and Table S1).

To determine whether AOPC metabolism can be realized by marine bacteria, environmental samples were collected at (1) the nature reserve in the Gulf of Eilat, Red Sea, Israel; and (2) three locations in the Mediterranean Sea, Israel. The Mediterranean Sea is particularly interesting because the concentration of labile phosphorous drops precipitously during the summer, below the uptake affinity of many organisms (19). The seawater samples were used to inoculate artificial seawater media containing 1 mM AOPC as the only P source and with various defined carbon sources (Fig. 2). Remarkably, all cultures exhibited growth on all tested AOPCs (compounds 8, 9, 10, and 12 in *SI Appendix*, Table S1, and compound 36 in Table S2, selected to have a range of chemical properties). Four serial passages of the cultures in liquid media resulted in the isolation of 17 bacterial strains from five orders of proteobacteria (Fig. 2 and *SI Appendix*, Table S3). The isolated strains are known to be abundant in the Mediterranean Sea (20) and the Red Sea (21), revealing that common bacteria (that are amenable to culturing techniques) in these environments are able to utilize several AOPCs as the sole source of P.

The ability of 20 different organophosphorus compounds (15 AOPCs and 5 products of their hydrolysis: diesters and their analogs) to support the growth of marine bacteria was assayed using 10 species from the isolated environmental strains (selected to maximize phylogenetic diversity) as well as four well-characterized marine bacteria: *Ruegeria pomeroyi* DSS-3 (22), *Ruegeria* sp. TM1040 (23), *Phaeobacter inhibens* (24), and *Dinoroseobacter shibae* (25) (Fig. 3 and *SI Appendix*, Figs. S2–S16). The patterns of AOPC utilization revealed two general trends: First, better leaving-group potentials support more robust bacterial growth (e.g., 4-hydroxy acetophenone); and second, almost all sources of P that were tested (with the exception of tributyl phosphate, compound 7), were metabolically accessible to the tested bacteria. Even nonactivated AOPCs, such as Tris(2-butoxyethyl) phosphate (compound 5; a widely used flame retardant in plastics and rubbers) could be harnessed as a source of P by five species in the absence of alternatives. The inability of *E. coli* to grow on any phosphotriesters serves as a reminder that PTE activity is not trivially present in all bacteria (14, 18, 26, 27).

Half of the tested bacterial species grew on phosphonate diesters (commonly used as nerve agents), suggesting the presence of a methylphosphonate utilization pathway, such as C-P lyases (28) or PhnY*/PhnZ oxygenases (29, 30), which convert methyl phosphonic acid to inorganic phosphate (Fig. 1). Genome analysis revealed that all phosphonate-utilizing strains, except *Alteromonas macleodii*, contain C-P lyase (as indicated by the presence of the *phn* operon and a PhnJ homolog with >70% sequence identity to the *E. coli* enzyme). *A. macleodii* contains a distant homolog of PhnY* with ∼30% sequence

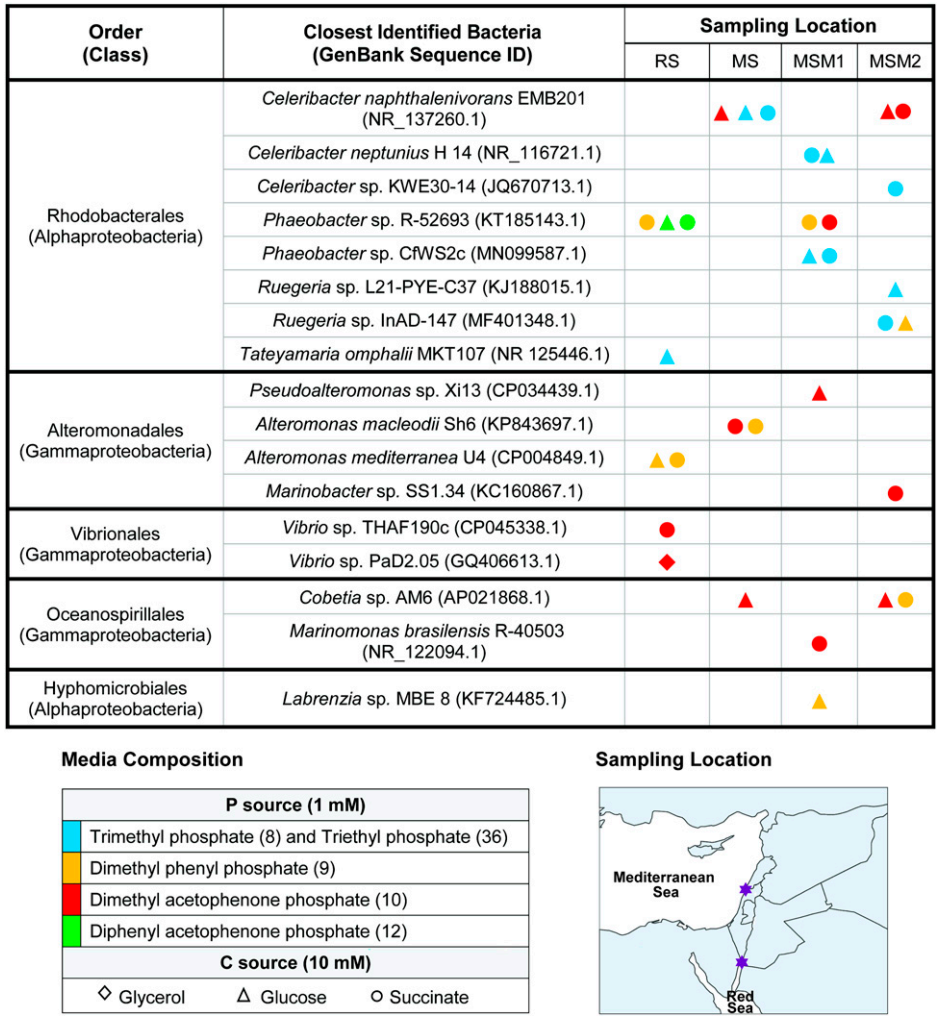

Fig. 2. Isolation and identification of marine bacteria that grow on organophosphates. Bacterial strains were isolated from the Red Sea and the Mediterranean Sea based on their ability to grow on various organophosphates as the sole P source (indicated in different colors). Different carbon sources were tested to maximize the number of strains isolated and included glycerol (indicated by diamonds), glucose (triangles) and succinate (circles). C, carbon; RS, Red Sea; MS, Mediterranean Sea, 600 m from the shore. Locations are specified in *Materials and Methods*.

identity to the characterized PhnY* from *Gimesia maris*. However, no PhnZ (the second oxygenase in the pathway) could be identified, so it remains unclear how *A. macleodii* utilizes phosphonates. Similarly, only distantly related homologs (~30% identity) of the phosphite dehydrogenase in *E. coli* could be identified in the profiled strains.

Identification of Two PTEs. While phosphatases and PDEs are widely distributed, few PTEs have been identified to date (14, 18, 26, 31). Given the potential value of novel PTE enzymes for bioremediation, we endeavored to identify which enzymes enabled growth on AOPCs. We focused on the two *Ruegeria* species (*R. pomeroyi* DSS-3 and *Ruegeria* sp. TM1040) because they can be easily cultured and exhibited robust growth on a variety of AOPCs but had different substrate preferences (*SI Appendix*, Fig. S17). Using PTE activity against chromogenic AOP analogs, in situ activity gels, and shot-gun proteomics (*SI Appendix*, Table S2 [compounds 24 to 29] and Fig. S18, and see *SI Appendix*, *Materials and Methods* for more details), two candidate genes encoding PTEs were identified. Both genes encode a periplasmic protein, which, given the proximity to the outer membrane, is consistent with the utilization of compounds present in the extracellular environment. The PTEs discovered in paraoxon and Tris(2-chloroethyl) phosphate contaminated soil are also periplasmic enzymes (27, 32). However, the genomic contexts of the putative PTE-encoding genes are not obviously related to the environmental acquisition of phosphorus (*SI Appendix*, Fig. S19).

To determine if expression of the putative PTE enzymes was up-regulated in the presence of AOPCs, both *Ruegeria* sp. were grown on media with either phosphate, dimethyl acetophenone phosphate (DMAP; compound 10) or diphenyl acetophenone phosphate (compound 12) as the P source. In phosphate-rich media, both genes exhibited basal expression levels similar to the housekeeping genes *gyrA*, *gyrB*, and *recA* (*SI Appendix*, Fig. S20). While expression of the putative PTE in the presence of AOPCs was largely unchanged for *Ruegeria* sp. TM1040, expression in *R. pomeroyi* DSS-3 increased 4-fold when grown on diphenyl acetophenone phosphate. This observed increase in gene expression suggests some degree of inducibility.

Although both PTEs originated from bacterial strains of the same genus, the enzymes themselves are nonhomologous, with one enzyme belonging to the metallo-β-lactamase superfamily (hereafter, MBL-PTE; National Center for Biotechnology Information reference sequence: WP_011538812.1) and the other enzyme belonging to the cyclase family (hereafter, cyclase-PTE; National Center for Biotechnology Information reference sequence: WP_011046510.1), identified in *Ruegeria* sp. TM1040

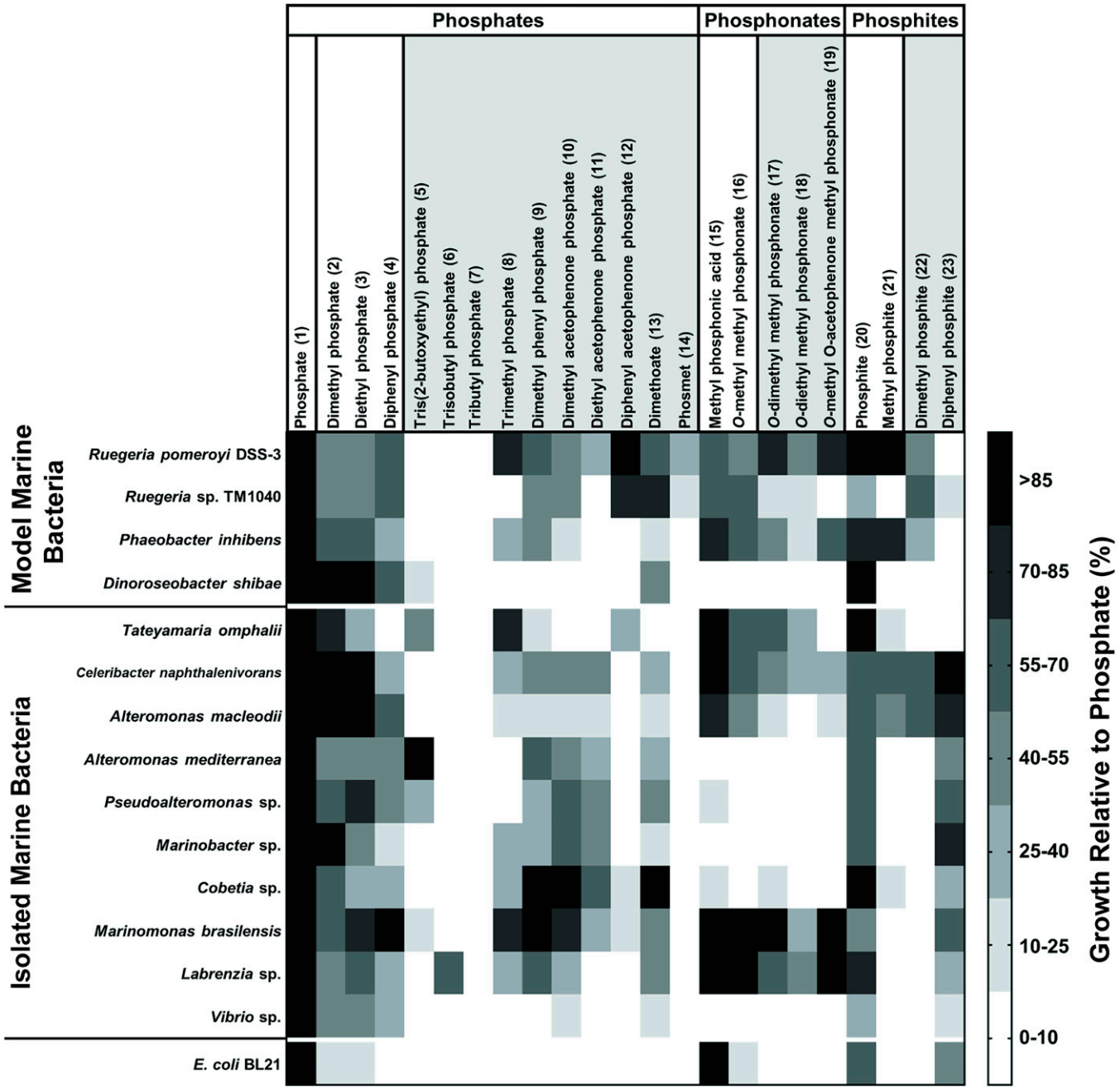

Fig. 3. Growth potential of model marine bacteria and environmental isolates on selected organophosphorus compounds. Compound numbers appear in parentheses and chemical structures can be found in *SI Appendix*, Table S1. See *SI Appendix*, Fig. S1 for a general description of the chemical properties of each compound. Anthropogenic chemicals (i.e., phosphotriesters and their analog phosphonate and phosphite diesters) are shaded in light gray. The growth potentials on each substrate were calculated from the maximum OD_{600} observed during growth on the substrate AOPC and normalized by the maximal OD observed during growth on phosphate. See *SI Appendix*, Figs. S2–S16 for the raw growth curves.

and *R. pomeroyi* DSS-3, respectively. Both of the purified gene products were confirmed to be active PTEs against multiple phosphotriesters (Fig. 4*A* and *SI Appendix*, Table S4). Furthermore, the catalytic efficiencies of the enzymes against various AOPCs are on par with or exceed that of the typical phosphoesterase (corresponding to Enzyme Commission [EC] numbers beginning with 3.1.3., 3.1.4., and 3.1.8.) in the Braunschweig Enzyme Database (BRENDA) of enzyme constants (Fig. 4*A* and *SI Appendix*, Table S4) (33). Neither enzyme has significant phosphatase or PDE activity, and both enzymes efficiently degrade lactones, as is common for PTEs (31, 34, 35) (Fig. 4*A* and *SI Appendix*, Figs. S21*A* and S22*A* and Table S4).

Next, we sought to explore whether PTE-encoding genes can be detected in the environment. A gene abundance analysis of the Tara dataset (36) found that these enzyme-encoding genes are common in the marine environment and present throughout the bacterial community (*SI Appendix*, Fig. S23). Likewise, an analysis of 52,515 genomes assembled from 7,304 metagenomes (37) indicates the presence of homologs of both the *R. pomeroyi* DSS-3 and *Ruegeria* sp. TM1040 putative PTEs in a variety of marine and terrestrial environments. MBL-PTE homologs were found in 3,116 metagenomes (n = 7,677 hits), while cyclase-PTE homologs were identified in 2,547 metagenomes (n = 4,494 hits) (Dataset S1).

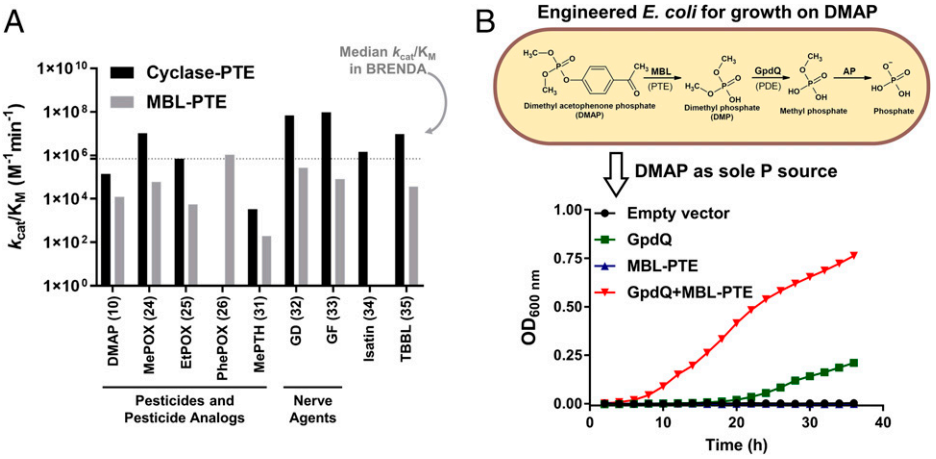

Fig. 4. Kinetic characterization of the newly discovered PTEs and engineering *E. coli* to utilize an AOPC as the sole P source. (*A*) The catalytic efficiency (k_{cat}/K_M) of cyclase-PTE from *R. pomeroyi* DSS-3 and the MBL-PTE from *Ruegeria* sp. TM1040 were determined for various AOPCs (e.g., pesticides, their analogs, and nerve agents). Each compound number appears in brackets and the structure can be found in *SI Appendix*, Table S1. The catalytic efficiency for the activity of the closest structural homologs was also measured (isatin for IH activity and thio-butyl-gamma-butyric lactone [TBBL] for lactonase activity). The dotted line indicates the median catalytic efficiency ($k_{cat}/K_M = 8.56 \times 10^6\ M^{-1}\ min^{-1}$) of all wild-type phosphoesterase-substrate pairs in BRENDA (Dataset S2). The values for each enzyme class are as follows: phosphatases ($n = 324$; median $k_{cat}/K_M = 1.1 \times 10^7\ M^{-1}\ min^{-1}$), PDEs ($n = 52$; median $k_{cat}/K_M = 1.8 \times 10^5\ M^{-1}\ min^{-1}$), and PTEs ($n = 23$; median $k_{cat}/K_M = 7.0 \times 10^5\ M^{-1}\ min^{-1}$). (*B*) Growth of *E. coli* BL21 coexpressing GpdQ and MBL-PTE in media with DMAP (compound 10) as the sole P source. Only coexpression of a PTE (MBL-PTE) and a PDE (GpdQ) resulted in robust growth on DMAP. Expression of GpdQ alone supported only modest growth, in accordance with the weak PTE activity of this enzyme (50).

PTE evolution within the metallo-β-lactamase superfamily has been previously observed, and MBL-PTE is related to previously discovered enzymes, all of which evolved from lactonases (*SI Appendix*, Fig. S24*A*). The closest known homolog of cyclase-PTE is isatin hydrolase (IH) (38) (*SI Appendix*, Fig. S24*B*), which, to our knowledge, has never before been associated with PTE activity. While cyclase-PTE retains IH activity (Fig. 4*A* and *SI Appendix*, Fig. S21*B*), it is at a lower level than the PTE activity against most of the tested phosphotriesters and phosphonate analogs (Fig. 4*A* and *SI Appendix*, Fig. S21 *C–H* and Table S4). IH enzymes do not generally exhibit PTE activity (*SI Appendix*, Fig. S25), suggesting that the *R. pomeroyi* DSS-3 enzyme was respecialized as a PTE. The respecialization may have involved a change in the catalytic metal, as IH activity was stimulated by Mn^{2+} whereas PTE activity was stimulated by Zn^{2+} in the growth medium (*SI Appendix*, Fig. S26) (38). Cyclase-PTE is also notable because, to our knowledge, this is the first wild-type enzyme that demonstrates high activity against the nerve agents soman (GD; compound 32 in *SI Appendix*, Table S2 and Fig. S21*C*) and cyclosarin (GF; compound 33 in *SI Appendix*, Table S2 and Fig. S21*D*). While previously discovered PTEs prefer the nontoxic R_P isomer or hydrolyze both the S_P and the R_P isomers with similar efficiency (39, 40), cyclase-PTE efficiently and preferentially hydrolyzes the neurotoxic S_P isomer (Fig. 4*A* and *SI Appendix*, Fig. S21 *C* and *D* and Table S4). Although the host organism, *R. pomeroyi* DSS-3, can grow on trimethyl phosphate (TMP), *O*-dimethyl methyl phosphonate (diMMPhn), and dimethyl phosphite (diMphosphite) (compounds 8, 17, and 22, respectively) (Fig. 3), we did not observe hydrolysis of these substrates by cyclase-PTE (*SI Appendix*, Fig. S27), suggesting an additional source of PTE activity.

To assess the bioremediation potential of PTE-encoding genes that were detected in the environment, we included representative homologs from marine, soil, and freshwater habitats in a phylogenetic analysis of MBL-PTE and cyclase-PTE (*SI Appendix*, Fig. S24 *C* and *D*). While all MBL-PTE homologs cluster with MBL-PTE, cyclase-PTE homologs are more distributed throughout the phylogenetic tree. Nevertheless, a majority of the homologous genes cluster around cyclase-PTE and isatin hydrolases. Although experimental confirmation is required, this analysis suggests that a diverse repertoire of genes that are distributed across environments have potential PTE activity.

Engineering *E. coli* to Grow on AOPCs. The in vitro characterizations of cyclase-PTE and MBL-PTE suggest that either enzyme, in concert with a PDE (Fig. 1), may be able to confer growth on an AOPC (Fig. 4*A* and *SI Appendix*, Table S4). To determine if PTE functionality can be readily incorporated into the metabolic repertoire of a naive bacterial strain, we coexpressed each of the two PTEs with a known PDE, GpdQ from *Enterobacter aerogenes* (41), in *Escherichia coli*. Previously, we observed that cyclase-PTE could not be efficiently expressed in *E. coli* and required coexpression with the chaperone GroELS (*SI Appendix*, Table S5). Under all conditions tested, cyclase-PTE expression was either detrimental or neutral to *E. coli* growth (*SI Appendix*, Fig. S28). Coexpression of MBL-PTE with GpdQ, on the other hand, dramatically improved the growth of *E. coli* on a medium with DMAP as the sole P source (Fig. 4*B*).

Conclusion

Mounting evidence suggests that phosphotriesters were not used by biological systems prior to their industrial production. For example, the Kyoto Encyclopedia of Genes and Genomes does not contain any natural phosphotriester metabolites (42). In light of the global distribution of AOPC pollutants (12, 13) and the associated environmental implications, unveiling the microbial capacity of and cellular machinery for metabolizing these compounds is crucial. In the present report, we demonstrate that a variety of marine bacteria can thrive on various AOPCs. In addition, we isolated two PTEs, one of which belongs to an enzyme family that, to the best of our knowledge, is unrelated to any PTE identified to date. The results presented herein suggest that the full breadth of AOPC utilization is underestimated and that man-made organophosphorus compounds have the potential to change the landscape of P utilization in marine ecosystems.

Materials and Methods

The synthesis of AOPCs is described in the *SI Appendix, Materials and Methods* section.

Isolation of Organophosphate-Degrading Bacteria from the Marine Environment. Seawater samples were taken from the Red Sea at the nature reserve in Eilat, Israel (pier IUI at 4 m depth, N 29.5035° E 34.9178°) on February 3, 2021, and from the Mediterranean Sea at the Achziv beach (N 33.0438°, E 35.1011°) on February 10, 2021. Three Mediterranean Sea samples were collected: The Mediterranean Sea sample was taken 600 m from the shore (density 1.0278 kg/L, temperature 22 °C, electrical conductivity [EC] 57.5 mS/cm, pH 6.48, dissolved oxygen [DO] 10.42 mg/L), while the Mediterranean Sea, coastal water mixed with fresh water at location 1 (MSM1) and Mediterranean Sea, coastal water mixed with fresh water at location 2 (MSM2) samples were collected at locations of lower salinity, where mixing of fresh water and seawater occurs (MSM1: 0 cm depth, ∼10 m offshore, density 1.0106 kg/L, temperature 21.7 °C, EC 25.6 mS/cm, pH 7.35, DO 6.27 mg/L; MSM2: 18 cm depth, ∼10 m offshore, density 1.0193 kg/L, temperature 19.7 °C, EC 37.1 mS/cm, pH 7.45, DO 3.22 mg/L). Water samples were passed through 40-μm filters and diluted 100-fold in 10 mL of artificial seawater media [ASW (43); note that 30 mM HEPES, instead of K_2HPO_4, was used for the basal medium] supplemented with AOPCs as the sole P source. One of four AOPC formulations was used: a mixture of 0.5 mM TMP and 0.5 mM triethyl phosphate (compounds 8 and 36, respectively); 1 mM dimethyl phenyl phosphate (compound 9); 1 mM DMAP (compound 10); or 1 mM diphenyl acetophenone phosphate (compound 12). Media were enriched with one of three different carbon sources: 10 mM glucose, succinate, or glycerol. Cultures were grown at 30 °C with continuous shaking at 220 rpm. Upon reaching optical density at a wavelength of 600 nm (OD_{600}) = 0.1 to 0.5, cultures were diluted into fresh media of the same composition. After four serial passages, cultures were streaked on Marine Broth agar plates containing phosphate and grown at 30 °C. Three colonies were picked from each plate for 16S ribosomal RNA (rRNA) amplification with the primers B_27_F (5′-AGAGTTTGATCCTGGCTCAG-3′) and U_1492_R (5′-GGTTACCTTGTTACGACTT-3′). The same three colonies were then used to reinoculate fresh media with the same composition as that used in the initial culture. Isolates were identified by 16S rRNA sequencing (*SI Appendix*, Table S3, Dataset S3) and stored in glycerol stocks. For further verification, the glycerol stocks were streaked on Marine Broth agar plates and grown overnight at 30 °C. Three new colonies were selected for 16S rRNA verification and stored in glycerol stocks.

Growth Profiling of the Isolated Marine Bacteria on Various AOPCs as the P Source. Single colonies were inoculated into Marine Broth and incubated at 30 °C overnight with continuous shaking at 200 rpm. Overnight cultures were washed twice with ASW media and the OD_{600} was adjusted to 1.0. Cultures were then diluted 100-fold in ASW media supplemented with 10 mM $CaCl_2$, basal media, bacterial vitamin mix (44), trace metal solution (45), 500 μM $NaNO_3$, 10 mM carbon source (the same one used for isolation), and 1 mM AOPC (substrates are listed in *SI Appendix*, Table S1, compounds 1 to 23) as the P source. All cultures were cultivated in 96-well microtiter plates. Each well contained 150 μL of culture covered with 50 μL of hexadecane to prevent evaporation (46). The OD_{600} was monitored by a plate reader (Epoch 2 Microplate Spectrophotometer; BioTek) every hour for 49 to 67 h with continuous shaking at 30 °C. Technical triplicates for the growth curves of *Celeribacter naphthalenivorans*, *A. macleodii*, *A. mediterranea*, *Vibrio* sp., and *Labrenzia* sp. were collected. Technical and biological triplicates were collected for *Cobetia* sp., *Marinobacter* sp., *Pseudoalteromonas* sp., *Marinomonas brasilensis*, and *Tateyamaria omphalii*. Both technical and biological replicates showed similar growth dynamics. All plots are of the mean value between the replicates with the error bars indicating the SDs. The maximum OD_{600} values were used to generate heat maps. Occasionally, wells showed the appearance of a second growth peak. Aggregates were evident in these wells; thus, the second peak likely appeared due to precipitation and/or cell aggregation in the microtiter plate. In these cases, values for the heat map in Fig. 3 were taken from the first peak, before the appearance of the second peak (examples are indicated by an arrow in *SI Appendix*, Fig. S7). Growth profiling of model marine bacteria and *E. coli* is described in *SI Appendix, Materials and Methods*.

Kinetic Characterization of PTEs: Cyclase-PTE and MBL-PTE. Isolation of PTEs, identification by mass spectrometry, cloning into *E. coli* expression vectors, recombinant expression, and purification are described in *SI Appendix, Materials and Methods*.

All activity measurements were performed in duplicate at 25 °C. Graphing and curve fitting was performed in GraphPad Prism 7 (GraphPad Software).

Activity buffers. The cyclase-PTE activity buffer comprised 50 mM Tris, 50 mM NaCl, and 0.1% Tergitol, at pH 8.0. The MBL-PTE activity buffer comprised 50 mM Tris, 50 NaCl, 1 mM $MnCl_2$, and 10% glycerol, at pH 8.0.

Caution. Concentrations of the in situ generated G and V nerve agents in diluted aqueous solutions are nonhazardous. Yet, due to their high potency as inhibitors of acetylcholinesterase (AChE), all safety requirements were strictly observed. The same practice should also be applied when working with the other organophosphates employed in this study.

Methyl paraoxon and paraoxon (compounds 24 and 25, respectively) hydrolysis. The release of *p*-nitrophenol during organophosphate hydrolysis was monitored at 405 nm and the Michaelis-Menten plot was obtained over 0.25 to 5 mM paraoxon and methyl paraoxon for MBL-PTE and over 0.025 to 1.5 mM paraoxon and methyl paraoxon for cyclase-PTE. Data points were analyzed by nonlinear regression analysis and k_{cat} was calculated using an extinction coefficient for *p*-nitrophenol at pH 8 of 1.6×10^4 M^{-1} cm^{-1}. The cyclase-PTE concentration was 1.6 nM for the methyl paraoxon and 16 nM for the paraoxon measurements; MBL-PTE concentrations were 0.42 μM for the methyl paraoxon and 0.83 μM for the paraoxon measurements.

Phenyl paraoxon (compound 26) hydrolysis. The release of *p*-nitrophenol during the hydrolysis of phenyl paraoxon was monitored at 405 nm and the Michaelis-Menten plot was obtained over 12.5 to 125 μM substrate for 84 nM MBL-PTE. Cyclase-PTE (15.9 μM) showed no release of *p*-nitrophenol with 0.2 mM substrate. Due to the low solubility of the substrate, 20% dimethyl sulfoxide was added to the reaction buffer.

Parathion and methyl parathion (compounds 30 and 31, respectively) hydrolysis. The release of *p*-nitrophenol during the hydrolysis of parathion and methyl parathion was monitored at 405 nm. Neither MBL-PTE nor cyclase-PTE hydrolyzed parathion. Samples with 8.3 μM MBL-PTE showed no release of *p*-nitrophenol with 0.2 mM parathion; likewise, samples with 15.9 μM cyclase-PTE showed no release of *p*-nitrophenol with 1.5 mM parathion. A Michaelis-Menten plot for the hydrolysis of methyl parathion by 15.9 μM cyclase-PTE was obtained over 0.1 to 1.5 mM substrate. The activity of 0.84 μM MBL-PTE was measured against 0.95 mM methyl-parathion.

GD and GF (compounds 32 and 33, respectively) hydrolysis. The in situ conversion of the coumarin surrogates of GD and GF to the corresponding G nerve agents in diluted aqueous solutions, as well as measurements of the rates of their detoxification by PTEs, was performed as previously described by Gupta et al. (47) and Ashani et al. (48). In these assays, the amount of residual nerve agent as a function of the incubation time with a PTE is measured by back titration with AChE.

Catalytic efficiencies (k_{cat}/K_M) for cyclase-PTE were determined by measuring the activity at several low GF (0.1, 0.5, and 1 μM) and GD (0.25 and 1 μM) concentrations in the approximated first-order kinetics region of the Michaelis-Menten equation. For the hydrolysis of 100 nM GF, the reaction was initiated by addition of 6.8 nM cyclase-PTE. At selected time intervals, aliquots were taken and diluted 20-fold in buffer containing 4 nM AChE in 50 mM Tris, 50 mM NaCl, and 0.1% Tergitol, at pH 8.0. The nearby stoichiometry of the inhibition of the AChE activity was completed within 60 to 80 min. In the case of GD, the reaction was initiated with 34 nM cyclase-PTE and, at selected time intervals, aliquots were taken and diluted 20-fold in 4 nM AChE in 50 mM Tris, 50 mM NaCl, and 0.1% Tergitol, at pH 8.0. The nearby stoichiometry of the inhibition of the AChE activity was completed within 80 to 120 min. The percentage of inhibited AChE without the cyclase-PTE was assigned a value of 100% residual GF. The decrease in the percent residual inhibitor was plotted versus the time of incubation and fitted to monoexponential decay kinetics (k_{obs}): $k_{cat}/K_M = k_{obs}/[\text{enzyme}]$.

Since MBL-PTE was, by far, less active in detoxification of GD (5 and 10 μM) and GF (10 μM), its concentration was increased to 0.84 μM for GD and 1.68 μM for GF. At specified time intervals, the reaction mixture was diluted 10- to 20-fold in 50 mM Tris, 50 mM NaCl, and 0.1% Tergitol, at pH 8.0 and then followed immediately by dilution into the AChE solution to determine the amount of residual nerve agent, as described above.

Isatin (compound 34) hydrolysis. The enzymatic hydrolysis of isatin to isatinate was monitored at 368 nm as described by Bjerregaard-Andersen (49). The isatin concentration ranged from 0.025 to 1.2 mM and the cyclase-PTE concentration was 0.16 μM. The data points were fitted to the Michaelis-Menten equation and analyzed by nonlinear regression. The k_{cat} was calculated using an extinction coefficient for isatinate at pH 8 of 4.5×10^3 M^{-1} cm^{-1}. MBL-PTE (0.55 μM) did not show activity when reacted with 0.69 mM isatin over 5 min.

Thio-butyl-gamma-butyric lactone hydrolysis (compound 35). The hydrolysis of thio-butyl-gamma-butyric lactone was followed using Ellman's reagent (5,5′-dithio-bis-[2-nitrobenzoic acid]) as described in Cherny et al. (40) at pH 8.0. A Michaelis-Menten plot for 34 nM cyclase-PTE was obtained over 0 to 0.14 mM substrate. A Michaelis-Menten plot for 0.42 μM MBL-PTE was obtained over 0 to 2.0 mM substrate.

VX (the S and R enantiomers, compound 40) hydrolysis. The hydrolysis of the toxic and less toxic VX enantiomers (S and R, respectively, at 0.01 to 0.02 mM) in the presence of 0.25 μM cyclase-PTE or 0.55 μM MBL-PTE was followed by Ellman's reagent. No release of the expected thiol leaving group could be observed after 10 min of incubation.

DMAP (compound 10) hydrolysis. The release of the leaving group *p*-hydroxy acetophenone was followed at 325 nm using a molar extinction coefficient at pH 8.0 of 1.52×10^4 M^{-1} cm^{-1}. A Michaelis-Menten plot was obtained over 0.2 to 3 mM DMAP using 0.16 μM cyclase-PTE. For 0.42 μM MBL-PTE, a concentration range of 0 to 1.72 mM DMAP was used.

AOPC Hydrolysis Monitored by ^{31}P NMR Spectroscopy. For hydrolysis of dimethyl phosphate (DMP), trimethyl phosphate (TMP), *O*-dimethyl methyl phosphonate (diMMPhn), *O*-methyl *O*-acetophenone methyl phosphonate (MAMPhn), and dimethyl phosphite (diMphosphite) (compounds 2, 8, 17, 19, and 22, respectively), cyclase-PTE was incubated with 5 mM DMP or TMP or with 10 mM diMMPhn, MAMPhn, or diMphosphite for up to 26 h at room temperature. The enzyme concentration was 250 nM for reactions with compounds DMP and TMP, 1 μM with MAMPhn, and 5 μM with diMMPhn and diMphosphite. A final concentration of 10% D_2O was added to the samples for reference. For DMP and TMP hydrolysis, pH was adjusted to 10 with 20 mM NaOH before the measurement. ^{31}P $\{^1$H$\}$ spectra were acquired, and chemical shifts are denoted in parts per million.

Data for MBL-PTE hydrolysis of 10 mM diMMPhn, MAMPhn, and diMphosphite monitored by ^{31}P NMR spectroscopy could not be acquired reliably due to the presence of $MnCl_2$ in the buffer.

Coexpression of PTEs (cyclase-PTE and MBL-PTE) with GpdQ PDE in *E. coli* BL21 and Growth on AOPC as the Sole P Source. Cells coexpressing cyclase-PTE with GroELS and cells expressing MBL-PTE were prepared as electrocompetent cells and each transformed separately with pET29b-GpdQ vector, which contains a PDE from *Enterobacter aerogenes* (50).

Cells coexpressing cyclase-PTE, GroELS, and GpdQ or MBL-PTE and GpdQ were inoculated into 5 mL of Luria-Bertani medium supplemented with 100 μg/mL ampicillin and 50 μg/mL kanamycin and grown overnight at 37 °C with shaking at 220 rpm. After overnight growth, the cells were washed two times with 3-(*N*-morpholino)propanesulfonic acid (MOPS) buffer at pH 7.4 and supplemented with 0.4% glucose, 1 mM isopropyl β-D-1-thiogalactopyranoside (IPTG), 0.5 mg/mL L-arabinose, and 5 μM K_2HPO_4. The cells were adjusted to $OD_{600} = 1$ and diluted 100-fold in 150 μL MOPS buffer at pH 7.4 supplemented with 0.4% glucose, 1 mM IPTG, 0.5 mg/mL L-arabinose, 5 μM K_2HPO_4, 0.1 mM $MnCl_2$, and 1 mM P source from the following: K_2HPO_4, DMP (compound 2), or DMAP (compound 10). Two additional P sources were used for the growth of cells expressing cyclase-PTE, GroELS, and GpdQ: MAMPhn (compound 19) and dimethyl phosphite (compound 22). For cyclase-PTE, the medium was also supplemented with 0.1 mM $ZnCl_2$. Each well was covered with 50 μL of hexadecane and the 96-well microtiter plate was incubated in a plate reader at 26 °C (cyclase-PTE) or 30 °C (MBL-PTE) for 69 h with continuous shaking.

Data Availability. All study data are included in the article and/or supporting information.

ACKNOWLEDGMENTS. We are grateful to Prof. Miguel Frada (The Hebrew University of Jerusalem) and Prof. Yael Kiro (Weizmann Institute of Science) for collecting water samples from the Red Sea and the Mediterranean Sea; Dr. Michael Etzerodt (Aarhus University) for sharing the isatin hydrolase gene; and Prof. Jonathan Todd (University of East Anglia) and Prof. Andrew Johnston (University of East Anglia) for kindly providing the *Ruegeria* strains. We acknowledge Roni Beiralas and Yemima Duchin Rapp for their assistance in establishing protocols for marine bacteria cultivation. We thank Dr. Shifra Ben-Dor for valuable discussions. We acknowledge insightful comments on the manuscript from Prof. Maria Vila-Costa, Prof. Ita Gruic-Sovulj, and Prof. Danica Galonić-Fujimori. D.D. and D.S.T. were supported by the Defense Threat Reduction Agency of the US Department of Defense (HDTRA1-17-0057). E.S. was funded by the Israeli Science Foundation (ISF 947/18), the Peter and Patricia Gruber Foundation, the Minerva Foundation with funding from the Federal German Ministry for Education and Research, the Angel Faivovich Foundation for Ecological Research, the Estate of Emile Mimran, and The Maurice and Vivienne Wohl Biology Endowment.

Author affiliations: [a]Department of Biomolecular Sciences, Weizmann Institute of Science, Rehovot 7610001, Israel; [b]Department of Chemical and Structural Biology, Weizmann Institute of Science, Rehovot 7610001, Israel; [c]Department of Plant and Environmental Sciences, Weizmann Institute of Science, Rehovot 7610001, Israel; [d]Dipartimento di Scienze Farmaceutiche, Università degli Studi di Milano, I-20133, Milano, Italy; [e]Nancy and Stephen Grand Israel National Center for Personalized Medicine, Weizmann Institute of Science, Rehovot 7610001, Israel; [f]Earth-Life Science Institute, Tokyo Institute of Technology, Tokyo 152-8550, Japan; and [g]Blue Marble Space Institute of Science, Seattle, WA 98104

Author contributions: D.D., L.M.L., E.S., and D.S.T. designed research; D.D., E.A., O.T., A.D., K.P.C., Y.A., O.E., A.C., and L.F. performed research; K.P.C., H.L., A.C., L.F., A.S., and Y.L. contributed new reagents/analytic tools; D.D., E.A., O.T., A.D., K.P.C., Y.A., O.E., M.S., L.M.L., E.S., and D.S.T. analyzed data; and D.D., L.M.L., E.S., and D.S.T. wrote the paper.

1. A. C. Martiny *et al.*, Biogeochemical controls of surface ocean phosphate. *Sci. Adv.* **5**, eaax0341 (2019).
2. S. Duhamel *et al.*, Phosphorus as an integral component of global marine biogeochemistry. *Nat. Geosci.* **14**, 359–368 (2021).
3. R. Feingersch *et al.*, Potential for phosphite and phosphonate utilization by Prochlorococcus. *ISME J.* **6**, 827–834 (2012).
4. S. S. Kamat, S. Singh, A. Rajendran, S. R. Gama, D. L. Zechel, *Enzymatic Strategies for the Catabolism of Organophosphonates* (Elsevier Ltd., ed. 3, 2020).
5. A. Martínez, M. S. Osburne, A. K. Sharma, E. F. DeLong, S. W. Chisholm, Phosphite utilization by the marine picocyanobacterium *Prochlorococcus* MIT9301. *Environ. Microbiol.* **14**, 1363–1377 (2012).
6. A. Martinez-Varela *et al.*, Bacterial responses to background organic pollutants in the northeast subarctic Pacific Ocean. *Environ. Microbiol.* **23**, 4532–4546 (2021).
7. M. Goldsmith *et al.*, A new post-intoxication treatment of paraoxon and parathion poisonings using an evolved PON1 variant and recombinant GOT1. *Chem. Biol. Interact.* **259** (Pt B), 242–251 (2016).
8. I. van der Veen, J. de Boer, Phosphorus flame retardants: Properties, production, environmental occurrence, toxicity and analysis. *Chemosphere* **88**, 1119–1153 (2012).
9. G.-L. Wei *et al.*, Organophosphorus flame retardants and plasticizers: Sources, occurrence, toxicity and human exposure. *Environ. Pollut.* **196**, 29–46 (2015).
10. F. Worek, H. Thiermann, T. Wille, Catalytic bioscavengers in nerve agent poisoning: A promising approach? *Toxicol. Lett.* **244**, 143–148 (2016).
11. M. Hu *et al.*, Regional distribution of halogenated organophosphate flame retardants in seawater samples from three coastal cities in China. *Mar. Pollut. Bull.* **86**, 569–574 (2014).
12. C. A. McDonough *et al.*, Dissolved organophosphate esters and polybrominated diphenyl ethers in remote marine environments: Arctic surface water distributions and net transport through Fram Strait. *Environ. Sci. Technol.* **52**, 6208–6216 (2018).
13. Y. Ma, Z. Xie, R. Lohmann, W. Mi, G. Gao, Organophosphate ester flame retardants and plasticizers in ocean sediments from the North Pacific to the Arctic Ocean. *Environ. Sci. Technol.* **51**, 3809–3815 (2017).
14. D. P. Dumas, S. R. Caldwell, J. R. Wild, F. M. Raushel, Purification and properties of the phosphotriesterase from *Pseudomonas diminuta*. *J. Biol. Chem.* **264**, 19659–19665 (1989).
15. K. Abe *et al.*, Haloalkylphosphorus hydrolases purified from *Sphingomonas* sp. strain TDK1 and *Sphingobium* sp. strain TCM1. *Appl. Environ. Microbiol.* **80**, 5866–5873 (2014).
16. M. Vila-Costa *et al.*, Microbial consumption of organophosphate esters in seawater under phosphorus limited conditions. *Sci. Rep.* **9**, 233 (2019).
17. H. Yamaguchi *et al.*, Phosphotriesterase activity in marine bacteria of the genera *Phaeobacter, Ruegeria*, and *Thalassospira*. *Int. Biodeterior. Biodegradation* **115**, 186–191 (2016).
18. A. Srivastava *et al.*, Enzyme promiscuity in natural environments: Alkaline phosphatase in the ocean. *ISME J.* **15**, 3375–3383 (2021).
19. T. F. Thingstad *et al.*, Nature of phosphorus limitation in the ultraoligotrophic eastern Mediterranean. *Science* **309**, 1068–1071 (2005).
20. R. Feingersch *et al.*, Microbial community genomics in eastern Mediterranean Sea surface waters. *ISME J.* **4**, 78–87 (2010).
21. G. A. Mustafa, A. Abd-Elgawad, A. Ouf, R. Siam, The Egyptian Red Sea coastal microbiome: A study revealing differential microbial responses to diverse anthropogenic pollutants. *Environ. Pollut.* **214**, 892–902 (2016).
22. C. R. Reisch *et al.*, Metabolism of dimethylsulphoniopropionate by *Ruegeria pomeroyi* DSS-3. *Mol. Microbiol.* **89**, 774–791 (2013).
23. S. L. Hogle, B. Brahamsha, K. A. Barbeau, Direct heme uptake by phytoplankton-associated *Roseobacter* bacteria. *mSystems* **2**, e00124-16 (2021).

24. E. Segev *et al.*, Dynamic metabolic exchange governs a marine algal-bacterial interaction. *eLife* **5**, e17473 (2016).
25. H. Wang, J. Tomasch, M. Jarek, I. Wagner-Döbler, A dual-species co-cultivation system to study the interactions between *Roseobacters* and dinoflagellates. *Front. Microbiol.* **5**, 311 (2014).
26. M. Goldsmith *et al.*, Evolved stereoselective hydrolases for broad-spectrum G-type nerve agent detoxification. *Chem. Biol.* **19**, 456–466 (2012).
27. S. Takahashi, H. Katanuma, K. Abe, Y. Kera, Identification of alkaline phosphatase genes for utilizing a flame retardant, tris(2-chloroethyl) phosphate, in *Sphingobium* sp. strain TCM1. *Appl. Microbiol. Biotechnol.* **101**, 2153–2162 (2017).
28. C. M. Chen, Q. Z. Ye, Z. M. Zhu, B. L. Wanner, C. T. Walsh, Molecular biology of carbon-phosphorus bond cleavage. Cloning and sequencing of the phn (psiD) genes involved in alkylphosphonate uptake and C-P lyase activity in *Escherichia coli* B. *J. Biol. Chem.* **265**, 4461–4471 (1990).
29. S. R. Gama *et al.*, An oxidative pathway for microbial utilization of methylphosphonic acid as a phosphate source. *ACS Chem. Biol.* **14**, 735–741 (2019).
30. O. A. Sosa, J. R. Casey, D. M. Karl, Methylphosphonate oxidation in *Prochlorococcus* strain MIT9301 supports phosphate acquisition, formate excretion, and carbon assimilation into purines. *Appl. Environ. Microbiol.* **85**, 1–12 (2019).
31. X.-J. Luo *et al.*, Switching a newly discovered lactonase into an efficient and thermostable phosphotriesterase by simple double mutations His250Ile/Ile263Trp. *Biotechnol. Bioeng.* **111**, 1920–1930 (2014).
32. P. Gorla, J. P. Pandey, S. Parthasarathy, M. Merrick, D. Siddavattam, Organophosphate hydrolase in *Brevundimonas diminuta* is targeted to the periplasmic face of the inner membrane by the twin arginine translocation pathway. *J. Bacteriol.* **191**, 6292–6299 (2009).
33. D. Davidi, L. M. Longo, J. Jabłońska, R. Milo, D. S. Tawfik, A bird's-eye view of enzyme evolution: Chemical, physicochemical, and physiological considerations. *Chem. Rev.* **118**, 8786–8797 (2018).
34. L. Afriat, C. Roodveldt, G. Manco, D. S. Tawfik, The latent promiscuity of newly identified microbial lactonases is linked to a recently diverged phosphotriesterase. *Biochemistry* **45**, 13677–13686 (2006).
35. O. Khersonsky, D. S. Tawfik, Chromogenic and fluorogenic assays for the lactonase activity of serum paraoxonases. *ChemBioChem* **7**, 49–53 (2006).
36. E. Villar *et al.*, The Ocean Gene Atlas: Exploring the biogeography of plankton genes online. *Nucleic Acids Res.* **46** (W1), W289–W295 (2018).
37. S. Nayfach *et al.*; IMG/M Data Consortium, A genomic catalog of Earth's microbiomes. *Nat. Biotechnol.* **39**, 499–509 (2021).
38. T. Sommer *et al.*, A fundamental catalytic difference between zinc and manganese dependent enzymes revealed in a bacterial isatin hydrolase. *Sci. Rep.* **8**, 13104 (2018).
39. Y. Ashani *et al.*, Stereo-specific synthesis of analogs of nerve agents and their utilization for selection and characterization of paraoxonase (PON1) catalytic scavengers. *Chem. Biol. Interact.* **187**, 362–369 (2010).
40. I. Cherny *et al.*, Engineering V-type nerve agents detoxifying enzymes using computationally focused libraries. *ACS Chem. Biol.* **8**, 2394–2403 (2013).
41. S. Y. McLoughlin, C. Jackson, J. W. Liu, D. L. Ollis, Growth of *Escherichia coli* coexpressing phosphotriesterase and glycerophosphodiester phosphodiesterase, using paraoxon as the sole phosphorus source. *Appl. Environ. Microbiol.* **70**, 404–412 (2004).
42. M. Kanehisa *et al.*, KEGG for linking genomes to life and the environment. *Nucleic Acids Res.* **36**, D480–D484 (2008).
43. C. Goyet, A. Poisson, New determination of carbonic acid dissociation constants in seawater as a function of temperature and salinity. *Deep-Sea Res. A, Oceanogr. Res. Pap.* **36**, 1635–1654 (1989).
44. J. M. González, F. Mayer, M. A. Moran, R. E. Hodson, W. B. Whitman, *Microbulbifer hydrolyticus* gen. nov., sp. nov., and *Marinobacterium georgiense* gen. nov., sp. nov., two marine bacteria from a lignin-rich pulp mill waste enrichment community. *Int. J. Syst. Bacteriol.* **47**, 369–376 (1997).
45. M. D. Keller, R. C. Selvin, W. Claus, R. R. L. Guillard, Media for the culture of oceanic ultraphytoplankton. *J. Phycol.* **23**, 633–638 (1987).
46. K. Sklodowska, S. Jakiela, Enhancement of bacterial growth with the help of immiscible oxygenated oils. *RSC Advances* **7**, 40990–40995 (2017).
47. R. D. Gupta *et al.*, Directed evolution of hydrolases for prevention of G-type nerve agent intoxication. *Nat. Chem. Biol.* **7**, 120–125 (2011).
48. Y. Ashani *et al.*, In vitro detoxification of cyclosarin in human blood pre-incubated ex vivo with recombinant serum paraoxonases. *Toxicol. Lett.* **206**, 24–28 (2011).
49. K. Bjerregaard-Andersen *et al.*, A proton wire and water channel revealed in the crystal structure of isatin hydrolase. *J. Biol. Chem.* **289**, 21351–21359 (2014).
50. E. Ghanem, Y. Li, C. Xu, F. M. Raushel, Characterization of a phosphodiesterase capable of hydrolyzing EA 2192, the most toxic degradation product of the nerve agent VX. *Biochemistry* **46**, 9032–9040 (2007).